Seabird assemblages, abundance, and distribution in the African sector of the southern Indian Ocean

A.B. Makhado[1,2,6✉], F.E. Dakwa[2], P.G. Ryan[2], M.J. Masotla[1], B.M. Dyer[1],
S.M. Seakamela[1], F.W. Shabangu[4,5], S. Somhlaba[4] and R.R. Reisinger[3]

[1] Oceans and Coasts, Department of Forestry, Fisheries and the Environment
Cape Town, South Africa.

[2] FitzPatrick Institute of African Ornithology, University of Cape Town
Cape Town, South Africa.

[3] School of Ocean and Earth Science, University of Southampton
Southampton, United Kingdom.

[4] Fisheries Management Branch, Department of Forestry, Fisheries and the Environment
Cape Town, South Africa.

[5] Mammal Research Institute Whale Unit, Department of Zoology and Entomology
University of Pretoria, Pretoria, South Africa

[6] College of Marine Sciences, Shanghai Ocean University
999 Huchenghuan Road, Pudong New District, Shanghai, 201306, China

Email: amakhado@dffe.gov.za

Abstract

Seabird distributions in the Southern Ocean are influenced by the location and accessibility of suitable breeding sites, but also by the environmental factors that influence the distribution and availability of their prey. For example, oceanic fronts, concentrate prey at their surface and therefore present important foraging areas for many seabirds. This study investigated the latitudinal distribution and abundance of seabirds in the African sector of the Southern Ocean. In particular, we investigated the relationship of seabird assemblages and densities to key biophysical environmental parameters (SST, sea surface height, bathymetry) and the main oceanic fronts.

There was a high density of seabirds north of the Subtropical Convergence (STC), which is situated at approximately 39°S, with declining densities farther south. There was latitudinal segregation between several species, e.g. black-browed albatross (*Thalassarche melanophris*) occurred north of the STC, and grey-headed albatross (*T. chrysostoma*) occurred to south of it. The Subantarctic Front (SAF) and the Antarctic Polar Front (APF) had less influence on seabird populations than the STC. Latitude was the greatest predictor of seabird assemblages and densities, reflecting environmental gradients in physical and biological parameters and their influences on prey distributions. Of the environmental parameters, sea surface temperature and bathymetry were the most important physical features influencing seabird assemblages. In particular, the density of seabirds north of STC declined with increasing sea surface temperature and had a negative relationship with bathymetry, with most seabirds occurring in shallower waters. In contrast, seabird density had a positive linear relationship with sea surface height. Relationships with other environmental parameters, such as wind, salinity and chlorophyll concentration (as a proxy for productivity), were less well-defined.

Résumé

La distribution des oiseaux marins dans l'océan Austral est influencée par l'emplacement et l'accessibilité des sites de reproduction appropriés, mais aussi par les facteurs environnementaux qui influencent la distribution et la disponibilité de leurs proies. Par exemple, les fronts océaniques concentrent les proies à leur surface et constituent donc des zones d'alimentation importantes pour de nombreux oiseaux de mer. Cette étude porte sur la distribution latitudinale et l'abondance des oiseaux de mer dans le secteur africain de l'océan Austral. Nous avons notamment étudié la relation entre les assemblages et les densités d'oiseaux marins, d'une part, et les principaux paramètres biophysiques de l'environnement (température de surface de la mer, hauteur de la surface de la mer, bathymétrie) et les principaux fronts océaniques, d'autre part.

Une forte densité d'oiseaux marins a été observée au nord de la convergence subtropicale (STC), située à environ 39°S, avec une diminution de la densité plus au sud. Une ségrégation latitudinale a été observée entre plusieurs espèces, par exemple l'albatros à sourcils noirs (*Thalassarche melanophris*) au nord du STC et l'albatros à tête grise (*T. chrysostoma*) au sud de celui-ci. Le Front subantarctique (FSA) et le Front polaire antarctique (FPA) ont moins d'influence sur les populations d'oiseaux marins que la convergence subtropicale. La latitude est le principal facteur prédictif des rassemblements et des densités d'oiseaux marins, reflétant les gradients environnementaux dans les paramètres physiques et biologiques et leurs influences sur la répartition des proies. Parmi les paramètres environnementaux, la température de surface de la mer et la bathymétrie sont les caractéristiques physiques les plus importantes influençant les assemblages d'oiseaux marins. En particulier, la densité des oiseaux marins au nord de la convergence subtropicale (STC) a diminué avec l'augmentation de la température de surface de la mer et présente une relation négative avec la bathymétrie, la plupart des oiseaux marins se trouvant dans des eaux moins profondes. En revanche, la densité des oiseaux marins présente une relation linéaire positive avec la hauteur de la surface de la mer. Les relations avec d'autres paramètres environnementaux, tels que le vent, la salinité et la concentration en chlorophylle (comme indicateur de la productivité), sont moins bien définies.

Абстракт

На распределение морских птиц в Южном океане влияют расположение и доступность подходящих мест гнездования, а также экологические факторы, влияющие на распределение и доступность их добычи. Например, океанические фронтальные структуры концентрируют добычу у своей поверхности и поэтому представляют собой важные кормовые зоны для многих морских птиц. В данном исследовании изучается широтное распределение и численность морских птиц в африканском секторе Южного океана. В частности, мы исследовали взаимосвязь между сообществами морских птиц и их плотностью, и ключевыми биофизическими параметрами окружающей среды (температура поверхности моря, высота поверхности моря, батиметрия), а также основными океаническими фронтами.

К северу от субтропической конвергенции (СТК), расположенной примерно на 39° ю.ш., наблюдалась высокая плотность морских птиц, которая уменьшалась по мере продвижения на юг. Несколько видов продемонстрировали межширотную сегрегацию. Например, чернобровый альбатрос (Thalassarche melanophris) встречался к северу от СТК, а сероголовый альбатрос (T. Chrysostom) — к югу от нее. Субантарктический фронт (САФ) и Антарктический полярный фронт (АПФ) оказывали меньшее влияние на популяции морских птиц, чем СТК. Широта была основным фактором, определяющим состав и плотность популяций морских птиц, отражая градации физических и биологических параметров окружающей среды и их влияние на распределение кормовых ресурсов. Из экологических параметров наиболее важными физическими характеристиками, влияющими на сообщества морских птиц, были температура поверхности моря и батиметрия. В частности,

плотность морских птиц к северу от СТК уменьшалась с повышением температуры поверхности моря и имела отрицательную зависимость от батиметрии, при этом большинство морских птиц встречалось в более мелких водах. Напротив, плотность морских птиц продемонстрировала прямую зависимость от высоты поверхности моря. Взаимосвязь с другими экологическими параметрами, такими как ветер, соленость и концентрация хлорофилла (как показатель продуктивности), была менее четко определена.

Resumen

La distribución de las especies de aves marinas en el Océano Austral depende en parte de la ubicación y la accesibilidad de sitios adecuados para la reproducción, pero también de factores medioambientales que influyen en la distribución y la disponibilidad de sus presas. Por ejemplo, los frentes oceánicos llevan a la concentración de presas en la superficie y, por tanto, constituyen importantes zonas de búsqueda de alimentación para muchas aves marinas. Este artículo estudia la distribución latitudinal y la abundancia de aves marinas en el sector africano del Océano Austral. En particular, se estudia la relación de los agrupamientos y densidades de aves marinas con parámetros medioambientales biofísicos clave (SST, altura de la superficie del mar, batimetría) y con los principales frentes oceánicos.

La densidad de aves marinas al norte de la Convergencia Subtropical (STC), situada aproximadamente a 39°S, es elevada, y disminuye hacia el sur. Varias especies presentan una segregación latitudinal, por ejemplo, el albatros ojeroso (*Thalassarche melanophris*) se da al norte de la STC, y el albatros de cabeza gris (*T. chrysostoma*), al sur. El Frente Subantártico (SAF) y el Frente Polar Antártico (APF) ejercen menos influencia sobre las poblaciones de aves marinas que la STC. La latitud es el factor predictivo de los agrupamientos y las densidades de aves marinas más importante, y refleja gradientes medioambientales de parámetros físicos y biológicos y la consiguiente influencia en la distribución de las presas. De los parámetros medioambientales, la temperatura de la superficie del mar y la batimetría son las características físicas más importantes que influencian los agrupamientos de aves marinas. En particular, la densidad de aves marinas al norte de la STC disminuye con el aumento de la temperatura de la superficie del mar y presenta una relación negativa con la batimetría, dándose la presencia de aves marinas principalmente en las aguas menos profundas. En cambio, la densidad de aves marinas tiene una relación lineal positiva con la altura de la superficie del mar. Las relaciones con otros parámetros ambientales, como el viento, la salinidad y la concentración de clorofila (como indicador indirecto de la productividad) están menos claramente definidas.

Introduction

Marine predators are useful focal organisms to study scale-dependent foraging behaviour in relation to environmental heterogeneity because of the wide spatial and temporal scales over which the abundance and distribution of their prey varies (Pinaud and Weimerskirch, 2007). The distribution of upper trophic level predators in the marine environment reflects the abundance and availability of their prey (e.g. zooplankton, krill, nekton and small fish), which in turn respond to lower trophic level processes (Hyrenbach et al., 2007). These, together with ocean currents, bathymetry and other physical and biological processes, promote the growth and retention of plankton, leading to spatial heterogeneity in the distribution of organisms, influencing the distribution of top predators such as seabirds (Pinaud and Weimerskirch, 2007). Top predators can therefore be used as indicators of localised areas of high biological production (Joiris et al., 2007, 2013).

Studies of seabirds' life at sea are essential to the comprehensive understanding of their foraging behaviour, distribution and assemblages, since many species spend most of their time at sea (Balance, 2007). At-sea data provide insights into the biology of individual species at several ecological scales, including distribution, abundance (particularly for species that are difficult to census at colonies) and species–habitat relationships, the relationships between distribution and physical/biological ocean characteristics (Balance, 2007). In addition, seabird distributions are influenced not only by oceanographic conditions (such as fronts and eddies that tend to concentrate potential prey) but also by the location and accessibility of suitable breeding sites (Bost et al., 2009; Commins et al., 2014). In particular, high relative abundance of seabirds often occurs at mesoscale features (< 100 km in diameter) associated with upwelling (Abrams, 1985; Commins et al., 2014) and at hydrodynamic features near the continental margin (Hoffman et al., 1981; Briggs et al., 1984; Abrams and Miller, 1986).

At-sea seabird data provide more easily identifiable and detectable insights into oceanic ecosystems. Seabirds are wholly dependent upon marine systems for food. They are highly mobile, thereby integrating environmental signals on large spatial scales, making them important indicator species (Balance, 2007; Commins et al., 2014; Hazen et al., 2019). Seabirds provide a potential model for the successful management of oceanic resources that can provide a mechanism for the conservation of other trans-habitat and transboundary species.

Although there have been advances in technology that have allowed unprecedented insights into the movements of marine predators (Watanabe and Papastamatiou, 2023), this is restricted to small samples of individuals and tends to be biased to specific life-history stages (mainly breeding adults). Direct observations at sea allow broad-scale distribution patterns to be assessed and thus augment understanding of the distribution of marine predators. This study reports the effect of environmental parameters on the density, distribution and abundance of seabirds in the African sector of the Southern Ocean.

Methods

We used data from the Atlas of Seabirds at Sea (AS@S), a citizen science programme collaboration between the Department of Forestry, Fisheries and the Environment (DFFE), BirdLife South Africa and the FitzPatrick Institute of African Ornithology, University of Cape Town. The AS@S database is an open-access website hosting data collected from vessels of opportunity, which follow a standard protocol for counting seabirds within the Southern Ocean (AS@S, 2023). We downloaded data from the area 30–55°S and 0–40°E, from 2016 to 2021. No data were collected in 2020 due to vessel operation restrictions during the COVID-19 lockdowns. Data in 2021 were recorded as point counts rather than transects; hence, to include 2021 and select dominant species, we jointly modelled the transect and point counts as presence and absence.

These data were augmented by transect counts aboard the *SA Agulhas II*, which undertakes an annual cruise between Cape Town and the Prince Edward Islands in April–May each year, Antarctica in December–February each year, and Gough Island in September–October, western Atlantic Ocean to resupply the research and weather station, and exchange overwintering teams. It is important to note that sampling efforts were only in summer months. This possibly affected the distributions of species modelled. For example, most great-winged petrels are observed in the warmer waters because they are not breeding during the surveys. Birds were observed from a variety of vessels and

locations (bridge, on top of the bridge, forecastle, and bow) depending on the ship used. Standardized (10 minutes) effort-based transect counts were used to observe seabird distribution, abundance and density. All birds were identified to species level or the lowest possible taxon within 300 m, in a 90° or 180° arc from the bow. Further details of methodologies used to collect seabird at sea data are reported in AS@S (2023).

Three oceanic fronts occur in the study area: the Subtropical Convergence (STC), the Subantarctic Front (SAF) and the Antarctic Polar Front (APF). Based on these fronts, seabird counts were analysed according to four distinct water masses and biogeographical zones defined by previous studies (Pollard et al., 2002; Force et al., 2015; Whitehead, 2017): i) the Subtropical Zone (STZ) north of the STC, ii) the Subantarctic Zone (SAZ) located between the STC and SAF, iii) the Polar Frontal Zone (PFZ) between SAF and APF, and iv) the Antarctic Zone south of APF. Frontal positions within the Southern Ocean were detected from sea surface height (SSH) values using methods adapted from Swart et al. (2010) and Carpenter-Kling et al. (2020).

Environmental data

To test the hypothesis that seabird distribution and density are influenced by environmental factors, in-situ and satellite remote-sensed oceanographic predictors (sea surface temperature (SST), SSH, sea surface salinity (SSS), wind speed, chlorophyll a concentration (CHL)) were downloaded from https://resources.marine.copernicus.eu/ (Table 1). Bathymetry was also considered a potential driver of seabird assemblage at 1 arc-minute spatial resolution. Seabird counts were matched to the environmental data's mean daily averages in their respective native spatial resolutions, using the mean centroid position of each transect section (henceforth, 'samples'). Compared to the 10-minute count transects, oceanographic data usually have low spatial resolutions with pixels/grid cells covering large areas; this could reduce the power of analyses to detect the relationships between seabird abundance, density (birds/km^2) and oceanographic data.

Table 1: Environmental variables used in analysis. Daily throughout the observation period

Variable	Abbreviation	Temporal Resolution	Spatial Resolution	Source
Sea surface temperature	SST	Daily	0.083° x 0.083°	GLOBAL_MULTIYEAR_PHY_001_030[a]
Sea surface height	SSH	Daily	0.125° x 0.125°	GLOBAL_MULTIYEAR_PHY_001_030[a]
Sea surface salinity	SSS	Daily	0.125° x 0.125°	GLOBAL_MULTIYEAR_PHY_001_030[a]
Bathymetry	Bathy		1 Arc-minute	GLOBAL RELIEF MODEL ETOPO 1[b]
Wind speed	Wind	Daily	0.25° x 0.25°	WIND_GLO_WIND_L4_REP_OBSERVATIONS_012_006[a]
Chlorophyll a concentration	CHL	Daily	0.25° x 0.25°	GLOBAL_MULTIYEAR_BGC_001_029[a]

a   Copernicus Marine Service Information (https://marine.copernicus.eu/)
b   NOAA National Centers for Oceanographic Information, global relief model (https://www.ngdc.noaa.gov/mgg/global/global.html)

Statistical Analysis

For determining seabird assemblages, samples in waters <1000 m deep were excluded to reduce the effect of attraction to land. Before analysis, seabird density and abundance data were transformed using Tukey's Ladder of Powers using function *transformTukey* in package *rcompanion* (Tukey, 1977; Mangiafico, 2024) in R (R Core Team 2022). It uses a Shapiro-Wilks test to calculate an arbitrary lambda value for the data which is closest to achieving normality, and the value is used to transform the data. Species recorded in fewer than five transects were excluded from analyses: flesh-footed shearwater (1), long-tailed jaeger (5), northern royal albatross (1), Salvin's prion (5), spectacled petrel (1), chinstrap penguin (2), greater crested tern (3), grey-backed storm petrel (2), grey-headed gull (2), king penguin (2), Leach's storm petrel (2), light-mantled albatross (2), brown skua (3), common tern (3), Antarctic tern (4), Manx shearwater (4). Biases existed in the identification of prions, given that they typically fly in huge groups, limiting appropriate distinction.

To determine evidence of species assemblage and recognise species that likely occur in the same samples, we calculated a Spearman's rank correlation similarity distance matrix of species density across all samples. This was visualised using an agglomerative, hierarchical cluster analysis to produce a dendrogram with Ward's minimum variance method (Murtagh and Legendre, 2014). To avoid the bias of arbitrary choosing of clusters in the absence of a priori groups, we significantly determined clusters at the 1% significance level (alpha = 99) with 1000 permutations using the similarity profile permutation test (SIMPROF, Clarke et al., 2008).

Analysis of similarity was carried out using function '*Anosim*' in package '*vegan*' to test the null hypothesis of no difference in groups of samples delimited by the oceanic fronts (biogeographic zones) within the Southern Ocean (Anderson and Walsh, 2013; Oksanen et al., 2020). A non-parametric multidimensional scaling (nMDS) allows for a 2-dimensional visualisation of the dissimilarity in sampled groupings. We used the nMDS model with a Bray Curtis similarity matrix in package '*vegan*' to explore differences in species distribution across a priori group of samples (Oksanen et al., 2020). The goodness of fit of the model was evaluated using a stress level criterion (Kruskal, 1964; Zhu and Yu, 2009).

Finally, to detect the existence of a non-linear relationship between seabird distribution and environmental predictor variables (Guisan et al., 2002) we used a generalised additive model (GAM) with the '*gam*' function in the R package '*mgcv*' (Wood, 2022). The models were fitted with a Gaussian error distribution. If effective degrees of freedom (edf) <1, the relationship was deemed linear. Remote-sensed satellite data had different spatial resolutions (Table 1) and to avoid multicollinearity and concavity across predictors, we ran univariate GAMs (including samples with depth <1000 m in analysis). Model diagnostics were assessed using the package '*Dharma*'.

Predictive modelling methods and data analysis

Oceanographic data were used to predict the distribution of birds, between 30 and 60°S and 0 to 50°E, with year as a factor. Seabirds were modelled as density on a logarithmic scale to prevent the effect of extreme outliers and to normalise the data. For selected species, seabirds were modelled as presence and absence (1,0). Survey data provide count and presence data, with mostly no absence data, hence, we selected a few seabird species, and the empty transects were used as absence data.

The predictive performance of a species distribution model is affected by spatial autocorrelation. Ecological data are usually clustered, such that observations close together are more similar than those that are farther apart. A Moran's I test was used to detect spatial autocorrelation in the dataset, with values between -1 (where if dissimilar values are close together, there is perfect dispersion and scattering in the dataset) and 1 (where if similar values are close together, there is perfect correlation and grouping in the dataset). Using the R package '*ape*' and function '*Moran.I*', we found that the data was significantly spatially autocorrelated (Moran's I =0.03. p-value< 0.05). Four models were selected to predict the distribution of seabird density and four selected seabird species (Paradis and Schliep, 2019). Two spatial general linear regression models were used with latitude and longitude modelled as spatially correlated random effects with a Matern covariance using package 'glmmfields' and 'spatMM' (Anderson et

al., 2020; Rousset et al., 2022). A global random forest model was used because it allows for the existence of spatial non-stationarity in data, using the machine learning 'h20' package (LeDell et al., 2022). A GAM was also used with latitude and longitude as smoothed effects with a Gaussian/kriging process smoothing term, using 'mgcv' package (Wood, 2022). For seabird density, all four models were run with a Gaussian distribution process, and for presence and absence, all four models were run with a binomial distribution.

Weighted averages were used to create a single ensemble model to boost accuracy and predictive performance. The weights for each model were calculated using machine learning through a neural network library with 'neuralnet' package (Fritsch et al., 2019). The weights for each model were also calculated using a general linear regression model and the output of two ensemble methods were compared, and the better-performing one was chosen for the ensemble. The GAM was used to determine the relationship between seabird distribution and oceanographic data, to account for a non-linear relationship between seabird density and oceanographic variables.

Model diagnostics and performance

The test dataset was used to determine the predictive performance, while the training dataset was used to train (fit) the model. Firstly, we ran the four spatial models for density and presence/absence using the training data, with the oceanographic variables as predictors. The models were used to predict seabird distribution on the test dataset. To determine the predictive performance of each model we compared the observed and the predicted values in the test dataset. Model diagnostics were carried out using package '*DHARMa*' and '*gam.check*' function for the GAM model in the 'mgcv' package (Hartig and Lohse, 2022; Wood, 2022). Diagnostic values, root mean square error (RMSE), R^2, correlation, mean absolute error (MAE) and area under receiver-operated characteristic curve (AUC) were used to assess the performance of each model in predicting the seabird distribution, by using the models created from the training data to predict the independent test data (Supplementary Figures S1-S9 and Supplementary Table S1-S5). After modelling seabird distribution with oceanographic data, we used oceanographic data to predict the distribution of seabirds from 2016–2021 (excluding 2020 because there were no observations made in that year), creating distribution maps for both density and probability of occurrence (presence/absence, 0/1) of selected seabirds between 30°S and 55°S and 0°E to 40°E grid scale. All data analyses were carried out in R (R Core Team, 2022).
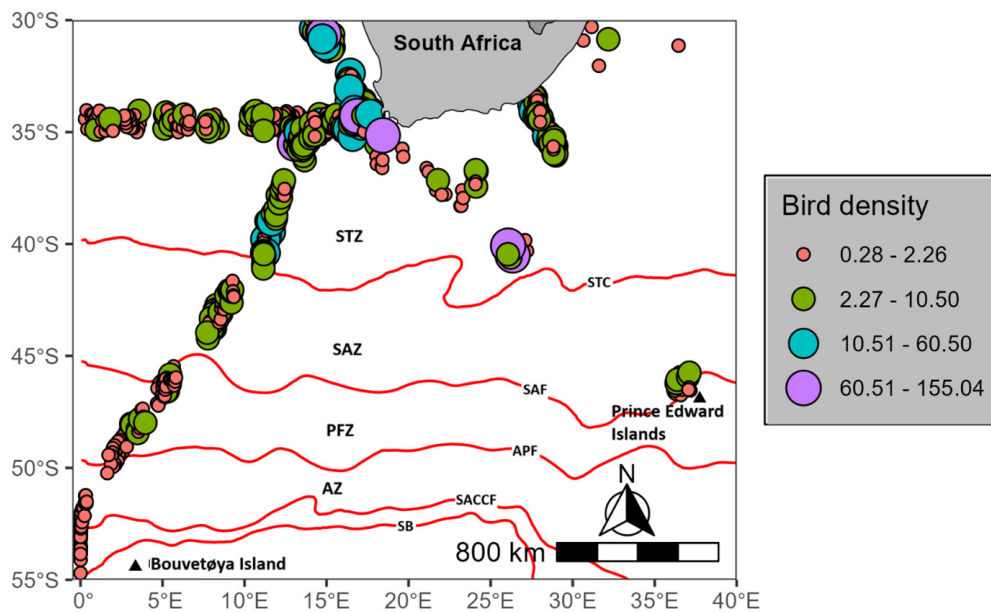

Figure 1: Distribution of seabird density throughout the study area. Mean locations of the Subtropical Convergence (STC), Subantarctic Front (SAF), Antarctic Polar Front (APF), Southern Antarctic Circumpolar Front (SACCF) and Southern Boundary (SB) are based on Orsi et al. (1995), dividing the Southern Ocean into the Subtropical Zone (STZ), Subantarctic Zone (SAZ), Polar Frontal Zone (PFZ) and the Antarctic Zone (AZ) south of the APF.

Results

We analysed 2284 transects, spanning a mean length of 3.4 ± 1.2 km, and covering a total of 77,893 km from 2016–2019. A total of 160 hours of seabird counts were made during the study period, recording 4,544 birds across 52 taxa (Table 2). Due to the opportunistic nature of the data used, the analysis had an unbalanced study design (uneven samples across groupings, spatial and temporal distribution). The highest seabird densities occurred within the STZ and the SAZ (Figures 1 and 2).

Seabird density increased from 3.7 birds/km^2 to 4.8 birds/km^2 from the STZ to the SAZ then reduced to 1.7 birds/km^2 and 0.7 birds/km^2 towards the PFZ and AZ, respectively (Table 2). The elevated seabird densities in STZ and SAZ came from the high numbers of Antarctic prions in the samples (Table 2; Figure 4). Seabird densities were binned according to 1° latitudinal sections and predictably there was high seabird density around the STC at ~39 S (Figure 3). Ten of the numerically dominant seabird species' densities were also binned into 1° latitudinal sections and spatial means calculated, showing spatial segregation in their latitudinal distribution and evidence of Antarctic prions peaking around the STZ and SAZ (Figure 4).
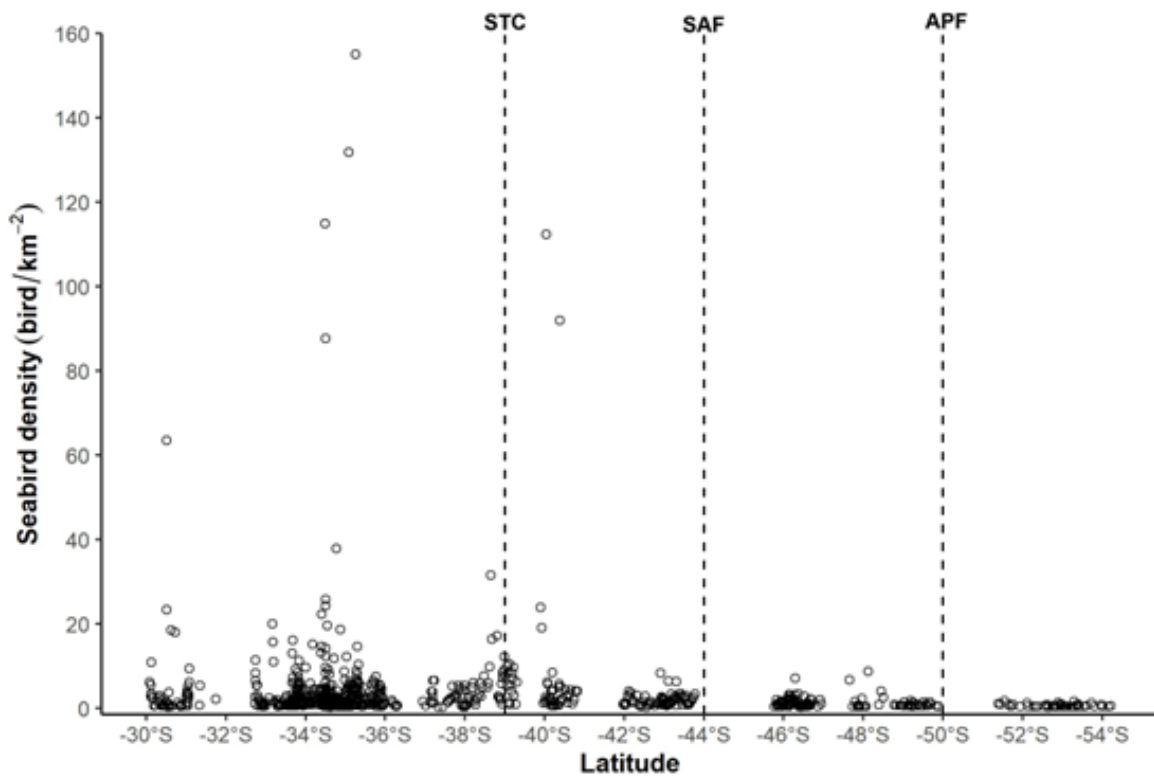

Figure 2: Seabird densities plotted along the latitudinal range along the study, dashed lines showing the latitudinal average position of Subtropical Front (STC), Subantarctic Front (SAF) and Antarctic Polar Front (APF).
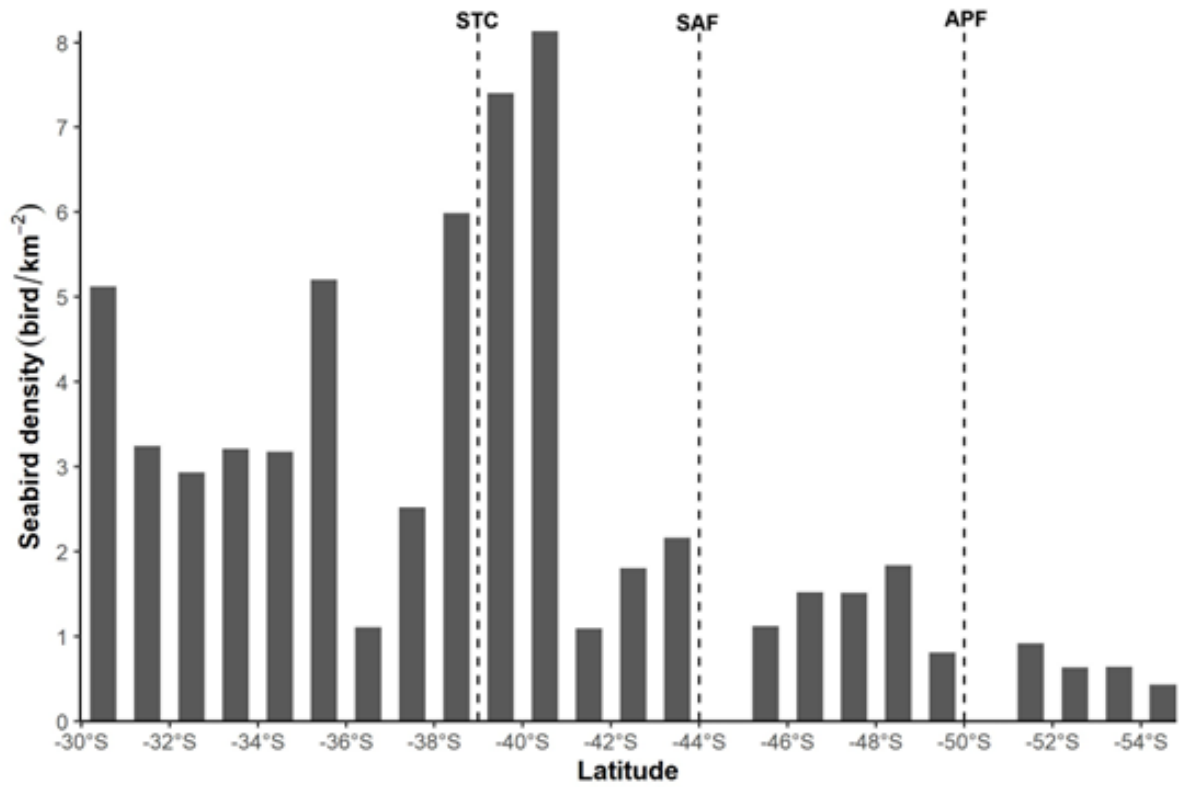
Figure 3: One-degree latitudinal spatial mean of total seabird densities. Dashed lines show the latitudinal average position of the Subtropical Front (STC), Subantarctic Front (SAF) and Antarctic Polar Front (APF).
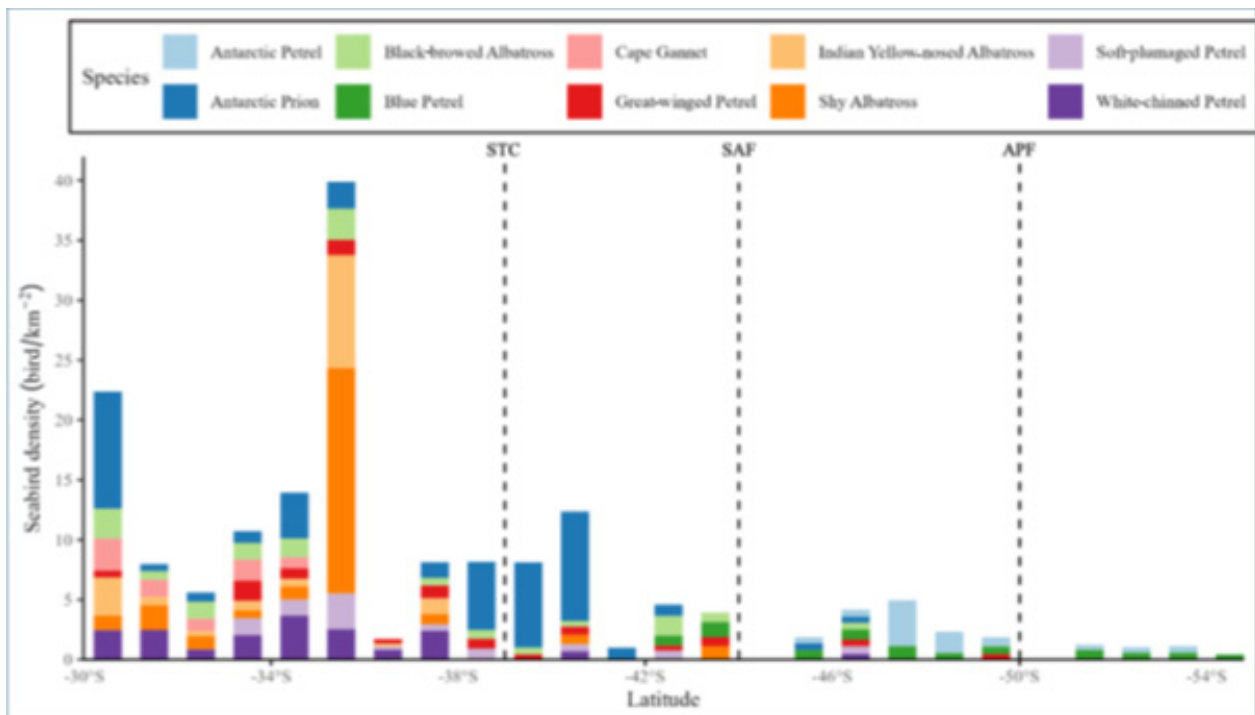

Figure 4: One-degree latitudinal spatial means of the 10 most abundant seabird species. Dashed lines show the average latitudinal position of the Subtropical Front (STC), Subantarctic Front (SAF) and Antarctic Polar Front (APF).

Table 2:   Abundance, density and frequency of occurrence (%) of seabird species throughout the study, along the transects sampled with the Southern Ocean from 2016-2019.

Biogeographic zone		STZ			SAZ			PFZ			AZ		
Common name	Scientific name	n	density	Freq (%)	n	density	Freq (%)	n	density	Freq (%)	n	density	Freq (%)
Grey-headed Gull	Chroicocephalus cirrocephalus	6	1.9	0.3	-	-	-	-	-	-	-	-	-
Kelp Gull	Larus dominicanus	30	1.5	1.9	-	-	-	-	-	-	-	-	-
Antarctic Tern	Sterna vittata	18	4.1	0.6	-	-	-	-	-	-	-	-	-
Arctic Tern	Sterna paradisaea	12	2	0.9	1	0.7	0.7	-	-	-	-	-	-
Common Tern	Sterna hirundo	7	1.5	0.5	-	-	-	-	-	-	-	-	-
Long-tailed Jaeger	Stercorarius longicaudus	5	1.8	0.2	-	-	-	-	-	-	-	-	-
Cape Gannet	Morus capensis	158	1.5	9.6	-	-	-	-	-	-	-	-	-
Antarctic Petrel	Thalassoica antarctica	-	-	-	-	-	-	64	1.2	23.2	8	0.5	15.6
Atlantic Petrel	Pterodroma incerta	4	0.5	0.6	19	0.7	13.3	1	0.7	0.9	-	-	-
Black-bellied Storm Petrel	Fregetta tropica	-	-	-	1	0.7	0.7	12	0.5	7.1	-	-	-
Blue Petrel	Halobaena caerulea	-	-	-	44	1.1	20.7	99	0.8	58.9	50	0.6	82.2
Common Diving Petrel	Pelecanoides urinatrix	-	-	-	-	-	-	11	0.6	8.9	-	-	-
European Storm Petrel	Hydrobates pelagicus	11	0.5	1.1	-	-	-	-	-	-	-	-	-
Great-winged Petrel	Pterodroma macroptera	226	1	23.1	14	0.6	10.4	8	0.5	6.2	-	-	-
Grey-backed Storm Petrel	Garrodia nereis	-	-	-	-	-	-	2	0.4	1.8	-	-	-
Grey Petrel	Procellaria cinerea	8	1.8	0.6	8	0.8	5.2	1	0.8	0.9	-	-	-
Kerguelen Petrel	Aphrodroma brevirostris	1	0.9	0.2	23	1.1	12.6	15	0.5	12.5	2	0.3	4.4
Leach's Storm Petrel	Hydrobates leucorhous	11	2	0.3	-	-	-	-	-	-	-	-	-
Northern Giant Petrel	Macronectes halli	5	0.5	0.8	-	-	-	3	0.4	2.7	-	-	-
Cape Petrel	Daption capense	28	1.6	2.3	9	0.8	5.2	4	0.7	2.7	-	-	-
Soft-plumaged Petrel	Pterodroma mollis	738	1.8	47.1	10	0.7	7.4	5	0.7	3.6	-	-	-
Southern Giant Petrel	Macronectes giganteus	6	0.8	0.8	9	0.9	5.2	12	0.6	8.9	7	0.5	13.3
White-chinned Petrel	Procellaria aequinoctialis	404	2.4	21.5	2	0.7	1.5	4	0.5	2.7	-	-	-
White-headed Petrel	Pterodroma lessonii	20	0.7	3.1	16	0.9	11.1	4	0.5	3.6	-	-	-
Wilson's Storm Petrel	Oceanites oceanicus	47	2.1	2.6	-	-	-	-	-	-	-	-	-
Chinstrap Penguin	Pygoscelis antarcticus	-	-	-	-	-	-	9	2	1.8	-	-	-
Antarctic Prion	Pachyptila desolata	590	2.9	22.3	665	7.2	37.8	3	0.6	2.7	-	-	-
Broad-billed Prion	Pachyptila vittata	-	-	-	24	16.4	0.7	-	-	-	-	-	-
Fairy Prion	Pachyptila turtur	-	-	-	-	-	-	18	0.9	6.2	-	-	-
Salvin's Prion	Pachyptila salvini	5	0.7	0.5	-	-	-	-	-	-	-	-	-
Slender-billed Prion	Pachyptila belcheri	-	-	-	37	1.8	6.7	-	-	-	-	-	-

Biogeographic zone			STZ			SAZ			PFZ			AZ		
Common name	Scientific name	n	density	Freq (%)	n	density	Freq (%)	n	density	Freq (%)	n	density	Freq (%)
Atlantic Yellow-nosed Albatross	Thalassarche chlororhynchos	58	2.9	4.8	-	-	-	-	-	-	-	-	-
Black-browed Albatross	Thalassarche melanophris	203	1.7	16.7	18	0.7	10.4	1	0.6	0.9	-	-	-
Grey-headed Albatross	Thalassarche chrysostoma	3	0.6	0.5	6	1.1	4.4	9	0.6	6.2	-	-	-
Indian Yellow-nosed Albatross	Thalassarche carteri	69	1.4	6.2	-	-	-	-	-	-	-	-	-
Shy Albatross	Thalassarche cauta	91	1.3	8.8	5	0.9	3	-	-	-	-	-	-
Sooty Albatross	Phoebetria fusca	14	0.7	2	5	1	3.7	4	0.4	3.6	-	-	-
Wandering Albatross	Diomedea exulans	18	1.9	2.5	4	0.7	2.2	4	0.5	3.6	-	-	-
Southern Fulmar	Fulmarus glacialoides	-	-	-	4	0.4	3	19	0.5	16.1	1	0.4	2.2
Cory's Shearwater	Calonectris borealis	50	2	2.6	-	-	-	-	-	-	-	-	-
Great Shearwater	Ardenna gravis	20	3.3	1.5	-	-	-	-	-	-	-	-	-
Subantarctic Shearwater	Puffinus elegans	3	0.6	0.5	5	0.7	3.7	-	-	-	-	-	-
Manx Shearwater	Puffinus puffinus	7	0.6	0.6	-	-	-	-	-	-	-	-	-
Sooty Shearwater	Ardenna grisea	33	1.1	3.3	2	0.6	0.7	-	-	-	-	-	-
Total samples			646			135			112			45		
Total birds			3102			1053			321			68		
Species richness			45			26			26			5		
Density (birds/km^2)			3.7			4.8			1.4			0.7		

Seabird assemblage

The SIMPROF test found significant evidence of internal structures within the seabird assemblages. Since SIMPROF does not assume any a priori groups, the test reveals that there are spatial differences among assemblages (across biogeographical zones) of seabirds. The clusters are evident in the dendrogram showing four main groups. Group (a) had 13 species with high-density aggregations in the warm waters of the STZ. Group (b) had two taxa, fairy prion and lack-bellied storm petrel, representative of the PFZ. Group (c) was characterised by six taxa with high densities south of the SAF within the PFZ and the AZ. The last group, (d), had species with the largest latitudinal range, occurring in waters stretching from the STZ to the north of APF, including 13 taxa (Figure 5; Table 2).

The results of the nMDS supported the clustering, showing that samples grouped according to biogeographic zones with overlaps between them (Figure 6). nMDS axis 1 showed substantial overlap across the groups, but nMDS axis 2 separated the samples across biogeographic zones (Figure 6). Stress for the two-dimensional nMDS was 0.004, indicating that the plot was an accurate representation of the sample's a priori group relationships. According to the ANOSIM, there was a significant difference in sample species assemblages across biogeographical zones (R = 0.28, p-value < 0.01). However, biogeographic zones only explained 8% of the variance in seabird assemblages. The GAM models showed that there was a non-linear relationship between environmental variables and seabird distribution (edf > 1). Latitude was the greatest predictor of seabird assemblages and densities, reflecting environmental gradients in physical and biological parameters, within and between water masses, and their influences on prey distributions. SST and bathymetry had the highest explanatory power (deviance explained). These results highlight the dynamic influence of oceanographic variables on the distribution of seabirds (Table 3; Figure 6).
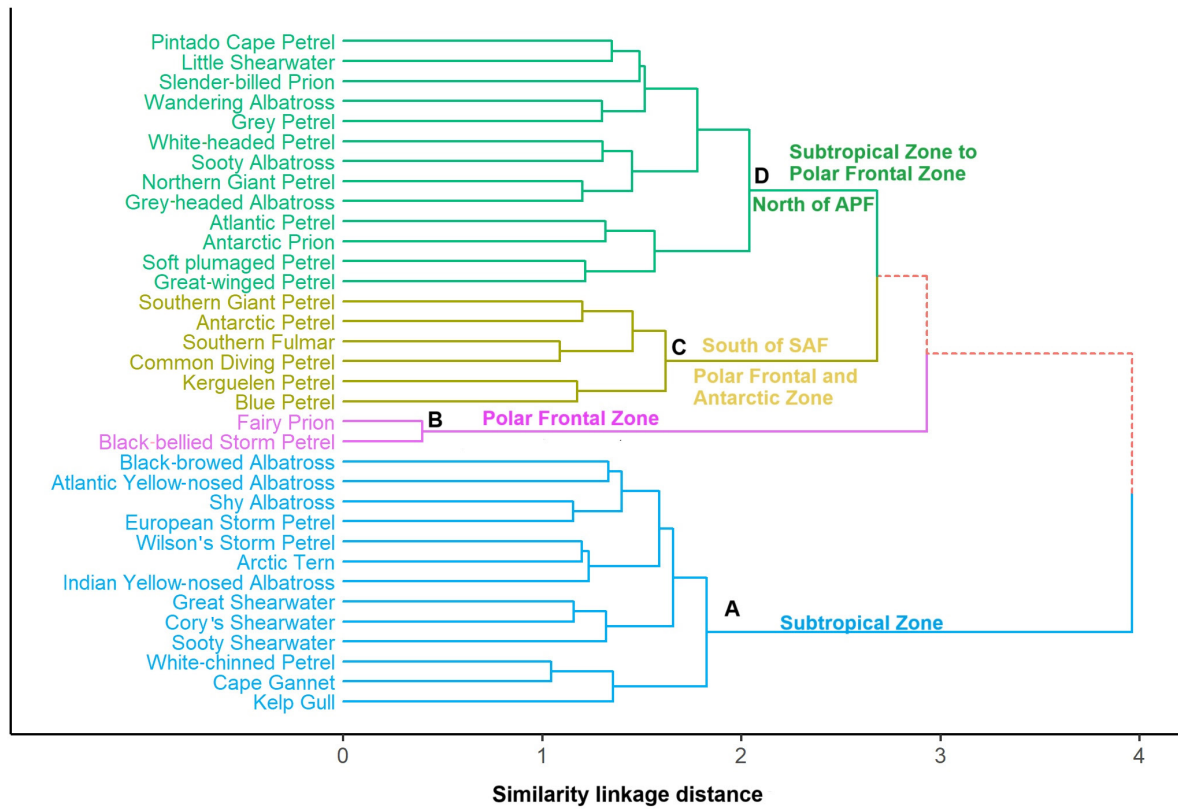
Figure 5: A dendrogram of seabird assemblages, along with SIMPROF test identifying significant clusters of seabird groupings. Four main groups were identified (A, B, C, D, colours) and distinguished according to the different biogeographic zones.
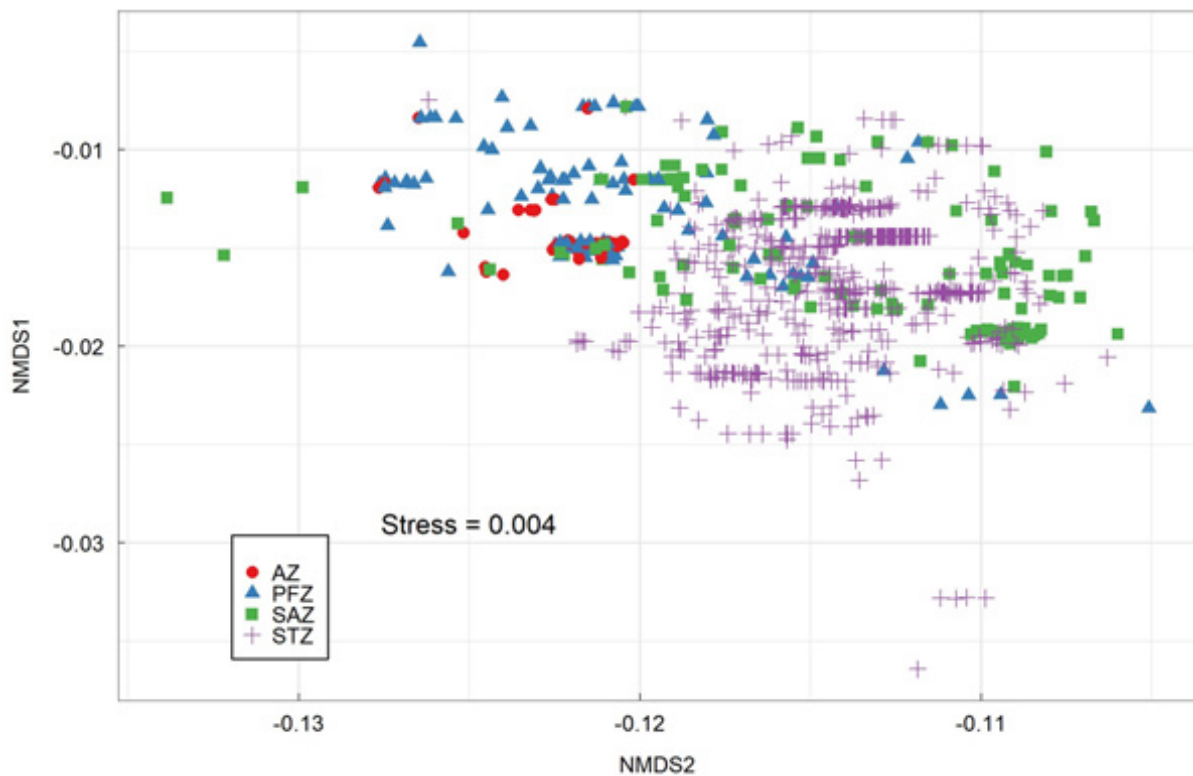

Figure 6: Non-parametric multi-dimensional scaling (nMDS) of seabird density assemblages grouped according to biogeographic zones: Subtropical Zone (STZ), Subantarctic Zone (SAZ), Polar Frontal Zone (PFZ) and Antarctic Zone (AZ)

Table 3:   Results of univariate generalised additive models (GAMs) of total seabird density against environmental variables; sea surface height (SSH), sea surface temperature (SST), chlorophyll-a (CHL), wind, ocean depth and latitude.

Variables	Edf	Ref. df	F-value	Deviance Explained (%)	P-value
SSH	7.1	8.09	17.29	13.00	<0.01
SST	8.6	8.96	19.23	16.00	<0.01
CHL	7.9	8.60	6.80	6.40	<0.01
Wind	8.6	8.90	12.60	11.00	<0.01
Bathymetry	8.6	8.90	6.60	6.04	<0.01
Latitude	6.2	7.30	22.00	15.00	<0.01
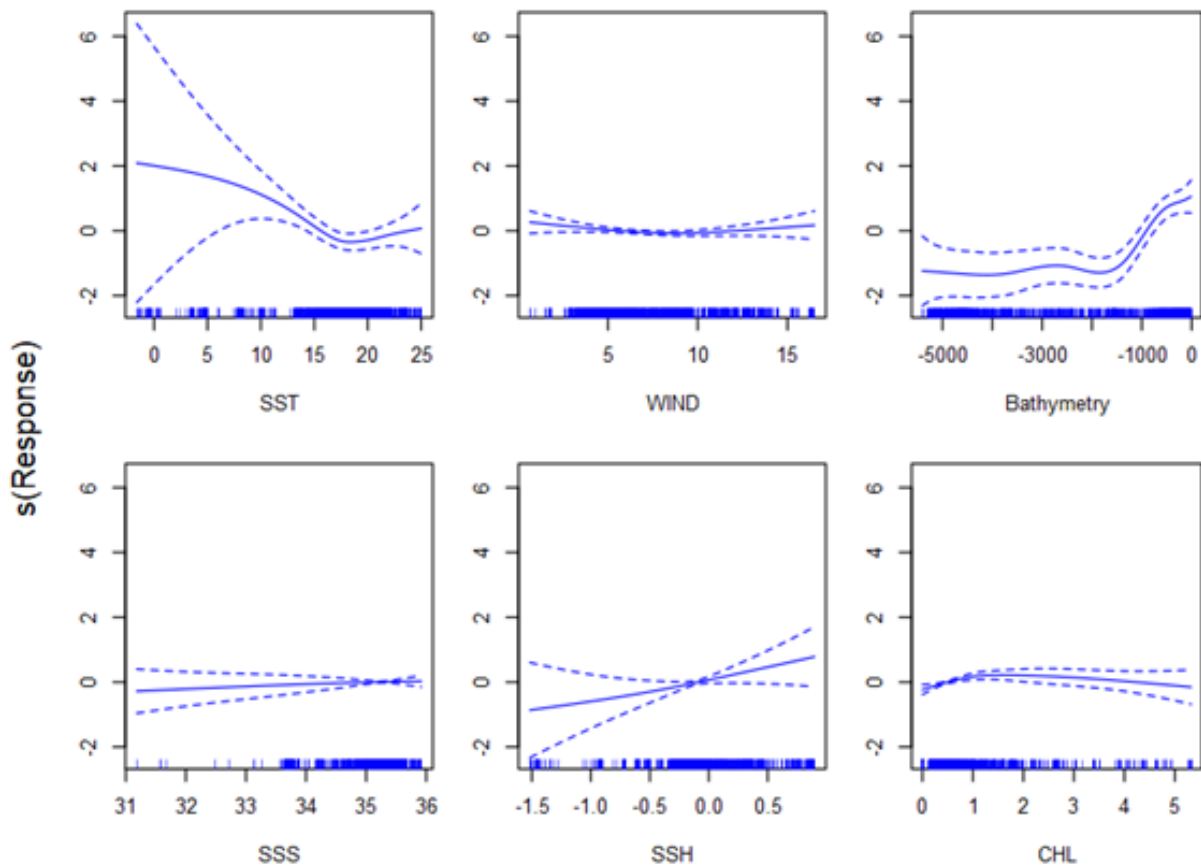
Figure 7:   Generalised additive model response curves showing the relationships between the density of all seabirds from 2016–2019 and oceanographic variables: sea surface temperature (SST), wind, bathymetry, sea surface salinity (SSS), seas surface height (SSH) and chlorophyll-a (CHL).

Seabird density relative to oceanographic variables

There was mostly a non-linear relationship between the oceanographic variables and the density of all seabirds. Seabird density reduced with increasing SST (GAM, edf = 3.39, F =1.83, p-value = 0.02, adjusted R^2 =0.48, deviance explained = 54%, Figure 2) and had a negative relationship with bathymetry (GAM, edf = 5.64, F = 6.33, p-value

<0.01, adjusted R^2 = 0.48, deviance explained = 54%, Figure 7). Seabird density had a positive but linear relationship (edf < 1) with SSH (GAM, edf = 0.91, F = 0.38, p-value <0.003, adjusted R^2 = 0.48, deviance explained = 54%, Figure 7). Relationships with other environmental parameters (wind, SSS and chlorophyll) were less defined. The presence of white-chinned petrels was variable, with low densities in 2015 but more abundant in 2016 and 2017.

Discussion

Within ocean ecosystems, biological resources are heterogeneous in distribution and abundance and depend to some degree on the physical characteristics of the water column (Bradshaw et al., 2004). Ocean fronts are not only the most important foraging areas for many top predators, but they also define the biogeographic boundaries for species in the Southern Ocean and play a critical role in structuring of seabird assemblages (Bost et al., 2009; Commins et al., 2013). Water masses and fronts, pack ice and ice margins, and eddies are some of the main hydrological factors explaining the distribution of seabirds in the ocean; this has been known for decades (Wynne-Edwards, 1935; Joiris, 1979; Pocklington, 1979; Kinder et al., 1983) and has been confirmed by for example Elphick and Hunt, 1993; Bost et al., 2009; Joiris and Falck, 2010 and this study. Seabird densities were highest within the STZ and SAZ, with their distribution and abundance closely linked to hydrographic features such as convergences, divergences, and fronts (Griffiths et al., 1982; Abrams, 1985; this study). In addition, seabird distributions are known to be influenced not only by oceanographic conditions that tend to concentrate potential prey, but also by breeding stages, the location and accessibility of suitable breeding sites (Cumming et al. 2013; Bost et al. 2009). It is therefore worth noting that during the period of observation, which was mainly in summer, and the resulting distribution applies to this time frame, as seabird activity and environmental conditions differ throughout the seasons.

Seabird densities increased from the STZ to the SAZ (from 3.7 birds/km^2 to 4.8 birds/km^2), and then decreased to 1.7 birds/km^2 and 0.7 birds/km^2 moving south to the PFZ and AZ. The waters between the STC and SAF support a diverse array of seabirds (this study). Sea surface temperature (SST) plays a key role in determining the biogeography and biogeochemistry of the Southern Ocean (Gibbons, 1997), particularly in the STC.

The structure of seabird communities south of Africa was best explained by latitude and SST. Both these variables reflect changes in physical factors within water masses, with resultant impacts on the distribution and abundance of prey species. SST and bathymetry were the most important physical factors determining seabird assemblages, which agrees with previous studies in other regions of the Southern Ocean (Ainley et al., 1994; Pinaud and Weimerskirch, 2007; Ribic et al., 2011; Commins et al., 2013). Latitude was the greatest predictor of seabird assemblages and densities, reflecting environmental gradients in physical and biological parameters, within and between water masses, and their influences on prey distributions. Due to the study design, we cannot attribute seabird assemblages to latitude only, but the presence of a relationship merits further study. These results highlight the dynamic influence of oceanographic variables on the distribution of seabirds while reflecting environmental gradients in both physical and biological parameters, within and between water masses, and their influences on prey distributions (Table 3; Figure 6). In contrast, seabird density had a positive linear relationship with sea surface height (SSH). This may be explained by their proclivity for frontal areas, which are characterised by increased SSH (Bradshaw et al., 2004). Relationships with other environmental parameters, namely wind, sea surface salinity and chlorophyll (as a proxy for productivity), were less defined.

The STC appears to serve as a significant demarcation for seabirds, acting as a biogeographical division between the Southern Ocean and the warmer subtropical waters to the north. The waters immediately north of the STC exhibit high productivity during both early and late summer (Laubscher et al., 1993; Barange et al., 1998). However, seabird densities generally remain low in the oceanic waters north of the STC. In contrast, the STC area shows high seabird densities, with prions being particularly abundant. Numerous species of albatrosses and petrels forage along the continental shelf of southern Africa. These include the more commonly encountered Atlantic and Indian yellow-nosed, black-browed and shy albatrosses, as well as the less common wandering albatross. While these species breed in the Subantarctic, as well as on islands off South America and Australasia, their overall contribution to the total sightings was negligible compared to the seabird's species breeding in coastal islands of South Africa. The presence of white-chinned petrels was variable, with low densities in 2015 but more abundant in 2016 and 2017.

Not all fronts have a significant impact on distinct zooplankton communities (Pakhomov et al., 2000) or seabird assemblages (Bost et al., 2009). The SAF and APF have less influence on seabird communities than the STC and ice-edge, and no clear structure was observed across the SACCF

during early summer (Bost et al., 2009). This is, however, important, especially that the subsequent distribution is primarily for the summer season during which this study was conducted, as seabird activity and environmental conditions vary throughout the year. Furthermore, most seabirds are concentrated in limited regions, which have well-defined boundaries in space and time. Abrams and Miller (1986) found considerably higher abundances of seabirds around the Prince Edward Islands compared to the STC or the Antarctic Polar Front south of Africa. Both these regions (islands off coast of South Africa and the Prince Edward Islands) have high densities of seabirds due to their proximity to breeding sites (Griffiths et al., 1982; Abrams, 1985a).

Aggregation of seabirds in these areas is likely due to the abundance of their prey and the position of fronts and water masses, which can vary greatly over small-time scales and thus influence seabird abundance. This study complements information from tracking studies (e.g., Reisinger et al., 2018; Hindell et al., 2020) in providing information on the distribution of seabirds at sea and the factors influencing their presence. This knowledge can greatly enhance the management and conservation efforts in the Southern Ocean through identifying those areas where seabirds congregate, which should be protected and conserved through international agreements such as Commission for the Conservation of Antarctic Marine Living Resources (CCAMLR). Measures like the establishment of marine protected areas in the high seas, which may include the CCAMLR Convention area, Area beyond National Jurisdiction and the continental shelf are crucial for promoting the sustainable use of marine resources and safeguarding the marine ecosystem.

Acknowledgments

References

Abrams, R.W. 1985. Environmental determinants of pelagic seabird distribution in the African sector of the Southern Ocean. *J. Biogeogr.*, 12: 473–492.

Abrams, R.W. and D.G.M. Miller. 1986. The distribution of pelagic seabirds in relation to the oceanic environment of Gough Island. *S. Afr. J. Mar. Sci.*, 4: 125–137.

AS@S. 2023. *Atlas of seabirds at sea*. Accessed from http://seabirds.saeon.ac.za/intro.aspx, 2023-1-26.

Ainley, D.G., C.A. Ribic and W.R. Fraser. 1994. Ecological structure among migrant and resident seabirds of the Scotia-Weddell confluence region. *J. Anim. Ecol.*, 63: 347–364.

Anderson, M.J. and D.C. Walsh. 2013. PERMANOVA, ANOSIM, and the Mantel test in the face of heterogeneous dispersions: What Null Hypothesis are you testing? *Ecol. Monogr.,* 83: 557–574. https://doi.org/10.1890/12-2010.1.

Balance, L.T. 2007. Understanding seabirds at sea: why and how? *Mar. Ornithol.*, 35: 127–35.

Barange, M., E.A. Pakhomov, R. Perissinotto, P.W Froneman, H.M. Verheye, J. Taunton-Clark, and M.I. Lucas. 1998. Pelagic community structure of the subtropical convergence region south of Africa and in the mid-Atlantic ocean. *Deep. Sea. Res. I.*, 45: 1663–1687.

Bradshaw, C.J.A., J. Higgins, K.J. Michael, S.J. Wotherspoon and M.A. Hindell. At-sea distribution of female southern elephant seals relative to variation in ocean surface properties. *ICES J. Mar Sci.*, 61 (6): 1014–1027. https://doi.org/10.1016/j.icesjms.2004.07.012.

Bost, C.A., C. Cotté, F. Bailleul, Y. Cherel, J.B. Charrassin, C. Guinet, D.G. Ainley and H. Weimerskirch. 2009. The importance of

oceanographic fronts to marine birds and mammals of the southern oceans. *J. Mar. Syst.*, 78: 363–376.

Briggs, K.T., K.F. Dettman, D.B. Lewis and W.B. Tyler. 1984. Phalarope feeding in relation to autumn upwelling off California. In: Nettleship, D.N., G.A. Sanger and P.F. Springer (Eds). *Marine Birds: their Feeding Ecology and Commercial Fisheries Relationships*. Canadian Ministry of Supply and Services, Ottawa: 51–62.

Carpenter-Kling, T., R.R. Reisinger, F. Orgeret, M. Connan, K.L. Stevens, P.G. Ryan, A. Makhado and P.A. Pistorius. 2020. Foraging in a dynamic environment: Response of four sympatric sub-Antarctic albatross species to interannual environmental variability. *Ecol. Evol.*, 10: 11277–95.

Commins, M.L., I. Ansorge and P.G. Ryan. 2014. Multi-scale factors influencing seabird assemblages in the African sector of the Southern Ocean. *Antarct. Sci.*, 26: 38–48.

Elphick, C., and G.L. Hunt, Jr. 1993. Variations in the distributions of marine birds with water mass in the Northern Bering Sea. *Condor*, 95: 33–44.

Fritsch, S., F. Guenther, M.N. Wright, M. Suling and S.M. Mueller. 2019. *Neuralnet: Training of Neural Networks*. https://github.com/bips-hb/neuralnet

Force, M.P., J.A. Santora, C.S. Reiss and V.J. Loeb. 2015. Seabird species assemblages reflect hydrographic and biogeographic zones within Drake Passage. *Polar Biol.*, 38: 381–392.

Gibbons, M.J. 1997. Pelagic biogeography of the south Atlantic Ocean. *Mar. Biol.*, 129: 757-68.

Griffiths, A.M., W.R. Siegfried and R.W. Abrams. 1982. Ecological structure of a pelagic seabird community in the Southern Ocean. *Polar Biol.*, 1: 39–46.

Guisan, A., T.C. Edwards, Jr and T. Hastie. 2002. Generalized linear and generalized additive models in studies of species distributions: setting the scene. *Ecol. Modell.,* 157 (2–3): 89–100.

Hartig, F. and L. Lohse. 2022. DHARMa: Residual Diagnostics for Hierarchical (Multi-Level/Mixed) Regression Models 90.4.50. https://CRAN.R-project.org/package=DHARMa.

Hazen, E.L., B. Abrahms, S. Brodie, G. Carroll, M.G. Jacox, M.S. Savoca, K.L. Scales, W.J. Sydeman and S.J. Bograd. 2019. Marine top predators as climate and ecosystem sentinels. *Front. Ecol. Environ.*, 17, 565–574. https://doi.org/10.1002/fee.2125.

Hindell, M.A., R.R. Reisinger, Y. Ropert-Coudert, L.A. Hückstädt, P.N. Trathan, H. Bornemann, J.-B. Charrassin, S.L. Chown, D.P. Costa, B. Danis, M.-A. Lea, D. Thompson, L.G. Torres, A.P. Van de Putte, R. Alderman, V. Andrews-Goff, B. Arthur, G. Ballard, J. Bengtson, M.N. Bester, A.S. Blix, L. Boehme, C.-A. Bost, P. Boveng, J. Cleeland, R. Constantine, S. Corney, R.J.M. Crawford, L. Dalla Rosa, P.J.N. de Bruyn, K. Delord, S. Descamps, M. Double, L. Emmerson, M. Fedak, A. Friedlaender, N. Gales, M.E. Goebel, K.T. Goetz, C. Guinet, S.D. Goldsworthy, R. Harcourt, J.T. Hinke, K. Jerosch, A. Kato, K.R. Kerry, R. Kirkwood, G.L. Kooyman, K.M. Kovacs, K. Lawton, A.D. Lowther, C. Lydersen, P.O. Lyver, A.B. Makhado, M.E.I. Márquez, B.I. McDonald, C.R. McMahon, M. Muelbert, D. Nachtsheim, K.W. Nicholls, E.S. Nordøy, S. Olmastroni, R.A. Phillips, P. Pistorius, J. Plötz, K. Pütz, N. Ratcliffe, P.G. Ryan, M. Santos, C. Southwell, I. Staniland, A. Takahashi, A. Tarroux, W. Trivelpiece, E. Wakefield, H. Weimerskirch, B. Wienecke, J.C. Xavier, S. Wotherspoon, I.D. Jonsen and B. Raymond. 2020. Tracking of marine predators to protect Southern Ocean ecosystems. *Nature*, 580: 87–92.

Hyrenbach, K.D., R.R. Veit, H. Weimerskirch, N. Metzl and G.L. Hunt. 2007. Community structure across a large-scale ocean productivity gradient: marine bird assemblages of the Southern Indian Ocean. *Deep Sea Res. I.*, 54: 1129–1145.

Hoffman, W., D. Heinemann and J.A. Wiens. 1981. The ecology of seabird feeding flocks in Alaska. *Auk*, 98: 437–456.

Joiris, C. 1979. Seabirds recorded in the northern North Sea in July: the ecological implications of their distribution. *Gerfaut*, 68: 419–440.

Joiris, C. 1983. Winter distribution of seabirds in the North Sea: an oceanological interpretation. *Gerfaut*, 73: 107–123.

Joiris, C.R. 2007. At-sea distribution of seabirds and marine mammals in the Greenland and Norwegian seas: impact of extremely low ice coverage. *Symposium European Research on Polar Environment and Climate, Brussels*, 5–6 March 2007. http://ec.europa. eu/research/environment/newsanddoc/agenda0307_en.htm.

Joiris, C.R. and E. Falck. 2010. Summer at-sea distribution of little auks *Alle alle* and harp seals *Pagophilus (Phoca) groenlandica* in the Greenland Sea: impact of small-scale hydrological events. *Polar Biol.,* 34: 541–548. https://doi.org/10.1007/s00300-010-0910-0.

Joiris, C.R., G.R. Humphries and A. de Broyer. 2013. Seabirds encountered along return transects between South Africa and Antarctica in summer in relation to hydrological features. *Polar Biol*., 36: 1633–47

Kinder, T.H., G.L. Hunt, Jr., D. Schneider and J.D. Schumacher. 1983. Correlations between seabirds and oceanic fronts around the Pribilof Islands, Alaska. *Estuar. Coast Shelf Sci*., 16: 309–319.

Kruskal, J.B. 1964. Multidimensional scaling by optimizing goodness of fit to a nonmetric hypothesis. *Psychometrika.,* 29: 1–27. https://doi.org/10.1007/BF02289565.

Laubscher, R.K., R. Perissinotto and C.D. McQuaid. 1993. Phytoplankton production and biomass at frontal zones in the Atlantic sector of the Southern Ocean. *Polar Biol.*, 13: 471–481.

LeDell, E., N. Gill, S. Aiello, A. Fu, A. Candel, C. Click, T. Kraljevic, T. Nykodym, P. Aboyoun, M. Kurka and M. Malohlava. 2020. H2O: R interface for the "H2O" scalable machine learning platform. https://github.com/h2oai/h2o-3.

Mangiafico, S.S. 2024. Rcompanion: Functions to Support Extension Education Program Evaluation. Rutgers Cooperative Extension, New Brunswick, New Jersey. version 2.4.35. https://CRAN.R-project.org/package=rcompanion/.

Murtagh, F. and P. Legendre. 2014. Ward's Hierarchical Agglomerative Clustering Method: Which Algorithms Implement Ward's Criterion? *J. Classif*., 31: 274–295. https://doi.org/10.1007/s00357-014-9161-z.

Pakhomov, E. and C. McQuaid. 1996. Distribution of surface zooplankton and seabirds across the Southern Ocean. *Polar Biol.,* 16: 271–286. https://doi.org/10.1007/s003000050054.

Paradis, E. and K. Schliep. 2019. ape 5.0: an environment for modern phylogenetics and evolutionary analyses in R. *Bioinformatics,* 35: 526–528.

Pinaud, D. and H. Weimerskirch. 2007. At-sea distribution and scale-dependent foraging behaviour of petrels and albatrosses: a comparative study. *J. Anim. Ecol*., 76: 9–19.

Pollard, R.T. M.L. Lucas and J.F. Read. 2002. Physical controls on biogeochemical zonation in the Southern Ocean. *Deep Sea Res II.*, 49: 3289–3305.

Pocklington, R. 1979. An oceanographic interpretation of seabird distributions in the Indian Ocean. *Mar. Biol.,* 51: 9–21.

R Core Team. 2022. R: A Language and Environment for Statistical Computing. R Foundation for Statistical Computing, Vienna. https://www.R-project.org.

Reisinger, R.R., B. Raymond, M.A. Hindell, M.N. Bester, R.J.M. Crawford, D. Davies, P.J.N. de Bruyn, B.J. Dilley, S.P. Kirkman, A.B. Makhado, P.G. Ryan, S. Schoombie, K. Stevens, M.D. Sumner, C.A. Tosh, M. Wege, T.O. Whitehead, S. Wotherspoon and P.A. Pistorius. 2018. Habitat modelling of tracking data from multiple marine predators identifies important areas in the Southern Indian Ocean. *Divers. Distrib.,* 24: 535–550.

Ribic, C.A., D.G. Ainley and L.B. Spear. 1997. Seabird associations in Pacific equatorial waters. *Ibis*, 139: 482–487.

Rousset F, J-B. Ferdy and A. Courtiol 2022. spaMM: Mixed-Effect Models, with or without Spatial Random Effects.

Swart, S., S. Speich, I.J. Ansorge and J.R. Lutjeharms. 2010. An altimetry-based gravest empirical mode south of Africa: 1. Development and validation. *J. Geophys. Res. Oceans*., 115(C3). https://doi.org/10.1029/2009JC005299.

Tukey, J. 1977. *Exploratory Data Analysis*. Addison-Wesley.

Oksanen, J., F.G. Blanchet, M. Friendly, R. Kindt, P. Legendre, D. McGlinn and H. Wagner. 2020. *vegan: Community ecology package [Computer software manual]*.

Watanabe, Y. Y. and Y. P. Papastamatiou. 2023. Biologging and biotelemetry: tools for understanding the lives and environments of marine animals. *Annu. Rev. Anim. Biosci.*, 11: 247–267.

Wynne-Edwards, V.C. 1935. On the habits and distribution of birds of the North Atlantic. *Proc. Boston Soc. Nat. Hist.,* 40: 233–346.

Whitehead, T.O., M. Connan, Y. Ropert-Coudert and P.G. Ryan. 2017. Subtle but significant segregation in the feeding ecology of sympatric penguins during the critical pre-moult period. *Mar. Ecol. Prog. Ser*., 17: 227–236.

Wood, S. 2022. Package 'mgcv': Mixed GAM Computation Vehicle with Automatic Smoothness Estimation. https://cran.r-project.org/web/packages/mgcv/mgcv.pdf.

Wood, S.N. 2011. Fast stable restricted maximum likelihood and marginal likelihood estimation of semiparametric generalized linear models. *J. R. Stat. Soc. Ser. B Stat. Methodol.*, 73 (1): 3–36. https://doi.org/10.1111/j.1467-9868.2010.00749.x.

Zhu, C. and J. Yu. 2009. Nonmetric multidimensional scaling corrects for population structure in association mapping with different sample types. *Genetics*, 182 (3): 875–888. https://doi.org/10.1534/genetics.108.098863.

Predicted seabird distribution of four most dominant seabirds species

The ensemble model performed better than individual models as it had low error (Table A1), and that model was used to produce the seabird density distribution map (Figure A1).

Table A1: Model diagnostic of observed vs predicted data deduced from the independent test data for the four models and the overall ensemble. RMSE (Root mean square deviation), R2 (Variance explained), Cor (Pearson correlation), MAE (mean absolute error).

Model	RMSE	R^2	Cor	MAE
GAM	1.03	0.43	0.66	0.79
GLMM	2.73	0.01	-0.11	2.17
SPMM	1.04	0.42	0.65	0.79
RF	0.96	0.50	0.65	0.75
Ensemble	0.91	0.56	0.75	0.69
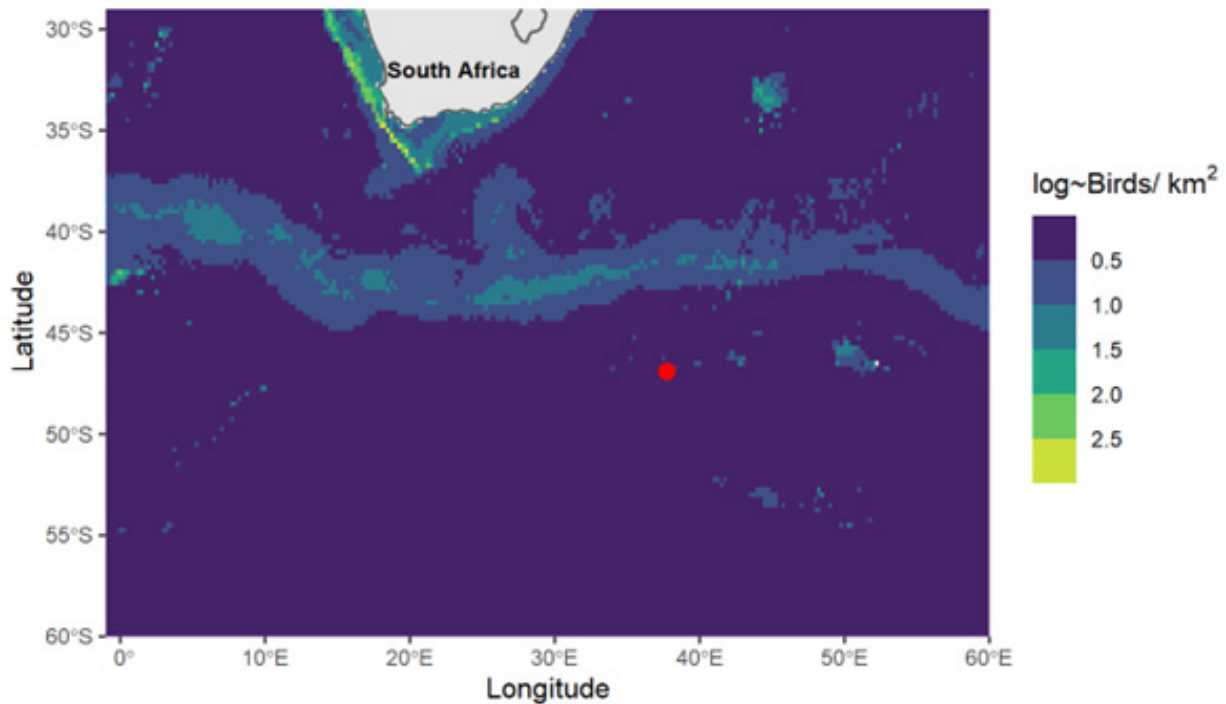
Figure A1: The predicted distribution of seabird density (birds/km2) from 2016–2021 (excluding 2020) from 300S to 600S and 00E to 600E, from the ensemble model. The location of the Prince Edward Islands is indicated by the red dot.

White-chinned petrel

White-chinned petrel probability of occurrence reduced with increasing SST (GAM, edf = 2.83, chi-square = 24.58, p-value <0.01, adjusted R^2 = 0.47, deviance explained = 46%, Figure A2, Table A2, Figure A3). Their probability of occurrence increased with reducing ocean depth (GAM, edf = 1.45, chi-square = 5.61, p-value = 0.01, adjusted R^2 = 0.47, deviance explained = 46%, Figure A2). There was no significant relationship between white-chinned petrel occurrence and chlorophyll a (GAM, edf = 0.0002, chi-square = 0.00, p-value = 0.68, adjusted R^2 = 0.47, deviance explained = 46%, Figure A2) and wind (GAM, edf = 0.0003, chi-square = 0.00, p-value = 0.63, adjusted R^2 = 0.47, deviance explained = 46%, Figure A2). White-chinned petrel probability of occurrence increased with SSH at low SSH and then reduced high SSH (GAM, edf = 2.91, chi-square = 15.41, p-value<0.01, adjusted R^2 = 0.47, deviance explained = 46%, Figure A2).
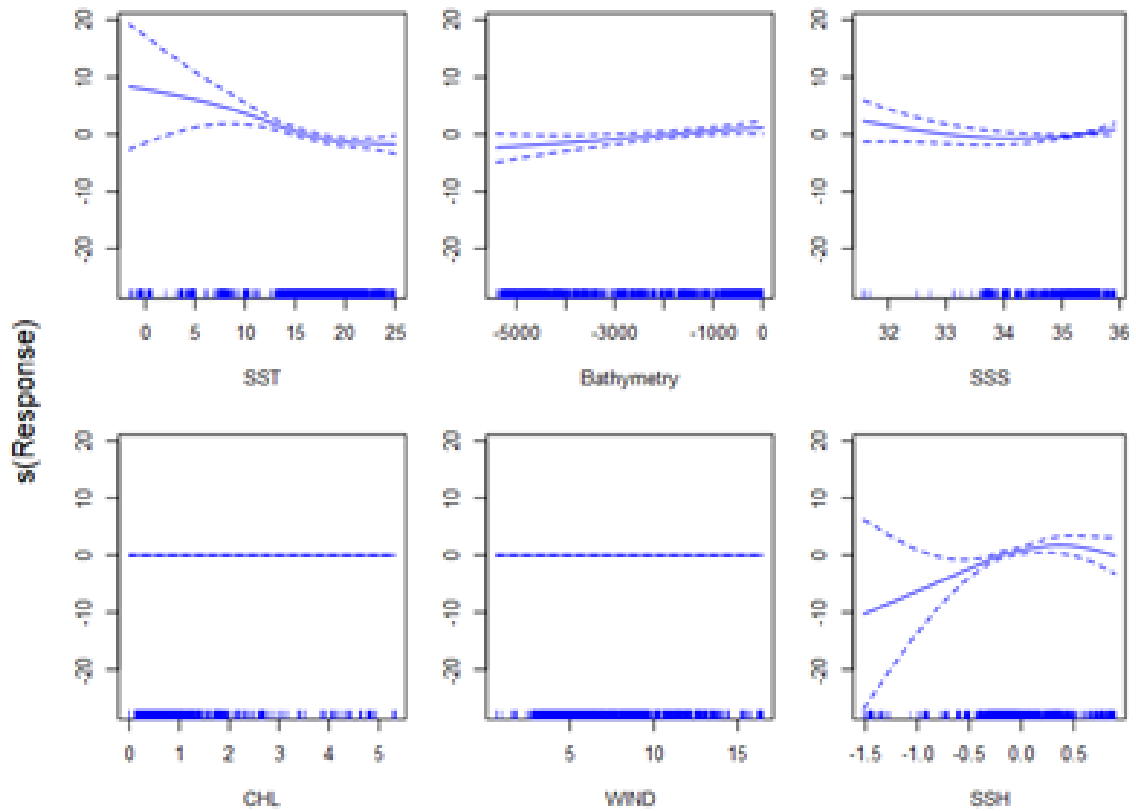
Figure A2: Response curves showing the relationship between the oceanographic variables and the probability of occurrence of white-chinned petrel 2016 – 2019, excluding 2020.

Model performance

Table A2: Model diagnostic of observed vs predicted white chinned petrel data deduced from the independent test data for the four models and the ensemble. RMSE (Root mean square error), R2 (Variance explained), Cor (Pearson correlation), AUC (Area under receiver-operated characteristic curve)

Model	RMSE	R^2	Cor	AUC
GAM	0.36	0.44	0.66	0.89
GLMM	0.43	0.24	0.49	0.78
SPMM	0.37	0.43	0.65	0.88
RF	0.35	0.47	0.68	0.90
Ensemble	0.34	0.47	0.68	0.92
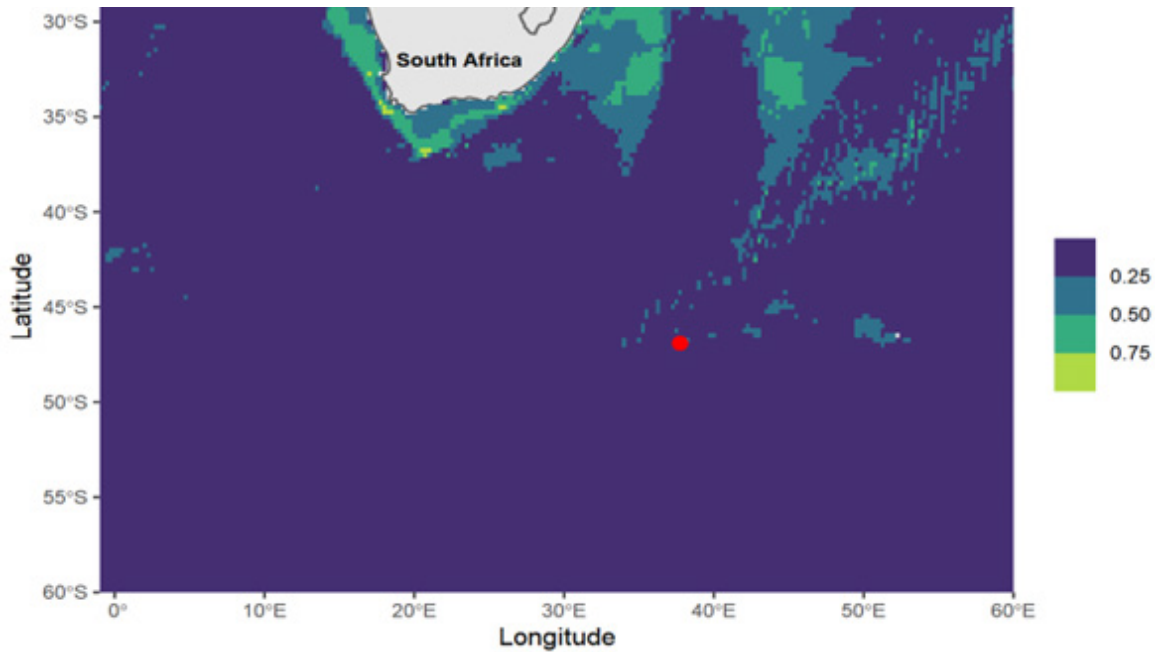
Figure A3: The predicted distribution (probability of occurrence) of white-chinned petrels from 2016-2021 (excluding 2020), using the ensemble model. The location of the Prince Edward Islands is indicated by the red dot.

Shy albatross

The probability of occurrence of shy albatrosses is reduced with increasing SST (GAM, edf = 1.27, chi-square = 9.27, p-value = 0.0003, adjusted R^2 =0.46, deviance explained = 49%, Figures A4 and A5, Table A3). There was a positive relationship between bathymetry and shy albatross (GAM, edf = 1.53, chi-square =8.57, p-value < 0.01, adjusted R^2 = 0.46, Deviance explained = 49%, Figure A4). Shy albatross probability of occurrence reduced with increasing sea surface salinity (GAM, edf = 1.07, chi-square = 5.98, p-value = 0.003, adjusted R^2 = 0.46, deviance explained = 49%, Figure A4). There was no significant relationship between shy albatross and chlorophyll a, wind and SSH (p-value > 0.05).

Model performance

Table A3: Model diagnostic of observed vs predicted shy albatross data deduced from the independent test data for the four models. RMSE (Root mean square error), R2 (Variance explained), Cor (Pearson correlation), AUC (Area under the receiver-operated characteristic curve).

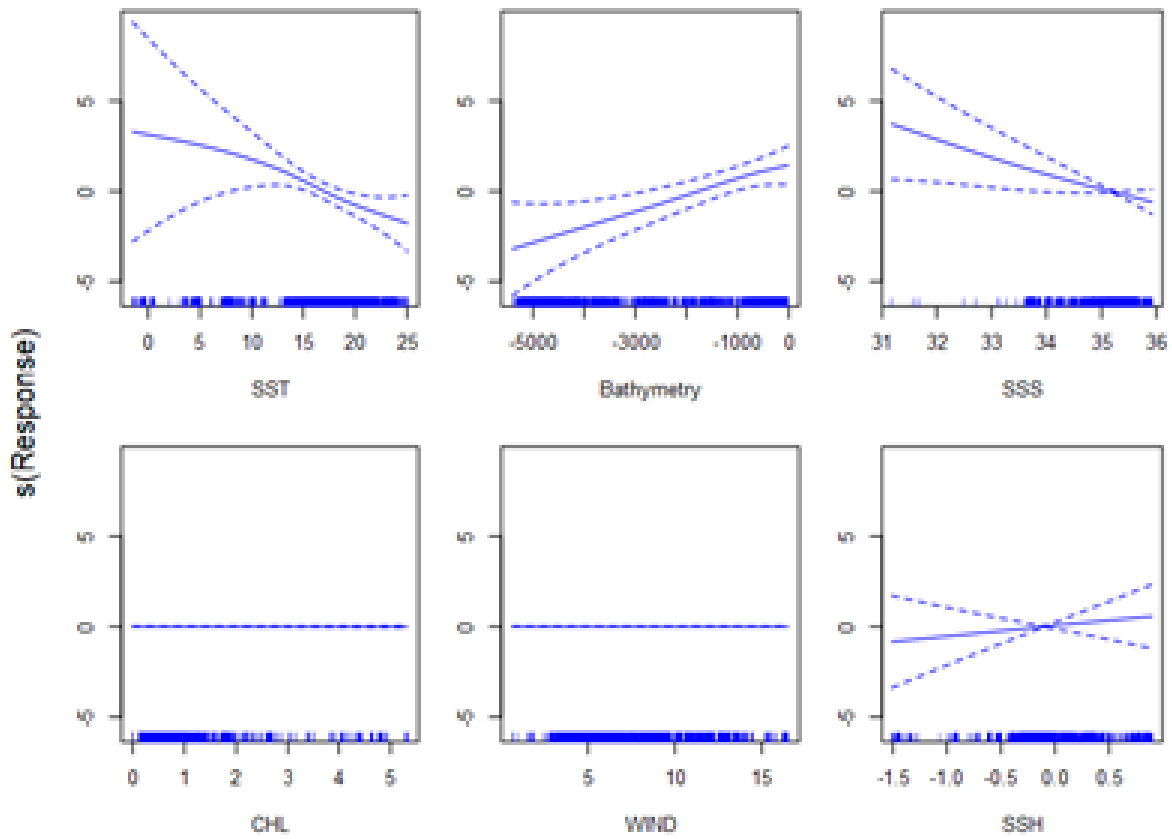| Model	RMSE	R^2	Cor	AUC
GAM	0.28	0.36	0.60	0.89
GLMM	0.33	0.16	0.40	0.80
SPMM	0.28	0.37	0.60	0.89
RF	0.24	0.45	0.68	0.95
Ensemble	0.23	0.62	0.79	0.97

Figure A4: Response curves showing the relationship between the oceanographic variables (sea surface temperature; SST, Wind, Bathymetry, sea surface salinity; SSS, seas surface height; SSH and Chlorophyll-a; CHL) and the probability of occurrence of shy albatross 2016 – 2021, excluding 2020.
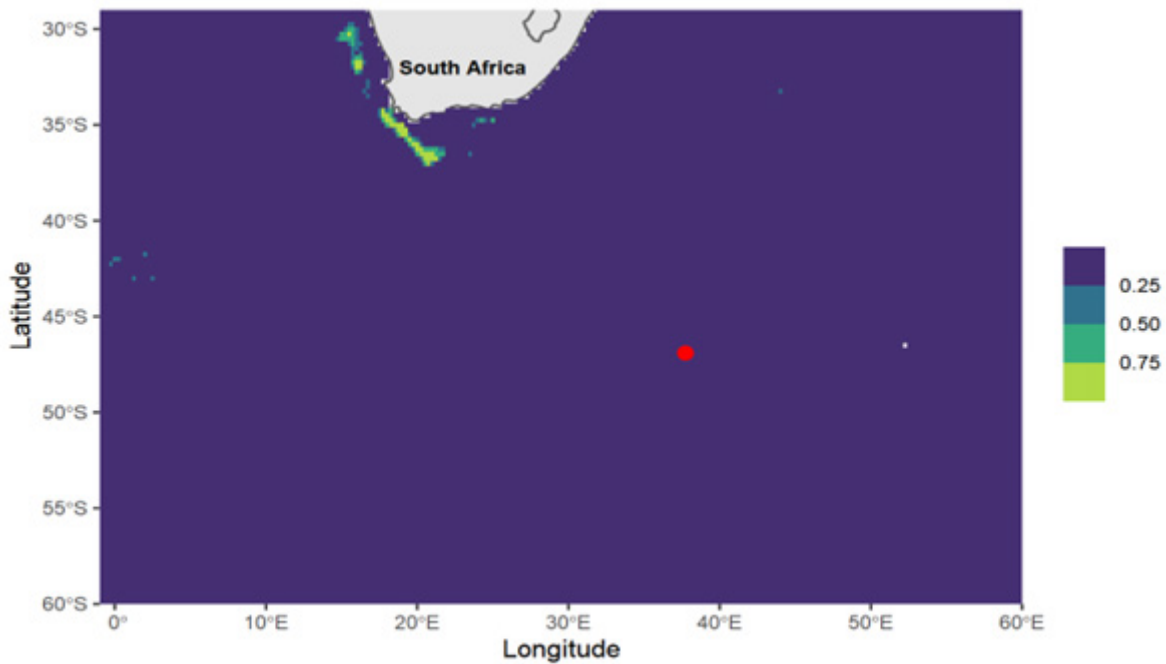

Figure A5: The predicted distribution (probability of occurrence) of shy albatross from 2016-2021 (excluding 2020) between 300S and 600S and 00E to 600E, from the ensemble model. The location of the Prince Edward Islands is indicated by the red dot.

Soft-plumaged petrel

Soft-plumaged petrel had a negative linear relationship (edf < 1) with SST (GAM, edf = 2.62, chi-square =1.58, p-value = 0.04, adjusted R^2 = 0.64, deviance explained = 66%, Figures A6 and A7, Table A4). Soft-plumaged petrel probability of occurrence reduced with increasing ocean depth; they occurred more in deeper waters (GAM, edf = 2.62, chi-square =15.74, p-value <0.01, adjusted R^2 = 0.64, deviance explained = 66%, Figure A6). Soft-plumaged petrel probability of occurrence increased with increasing wind speed (GAM, edf = 1.67, chi-square =5.17, p-value <0.01, adjusted R^2 = 0.01, deviance explained = 66%, Figure A6) and SST (GAM, edf = 0.85, chi-square = 3.195, p-value =0.003, adjusted R^2 = 0.64, deviance explained = 66%, Figure A6).
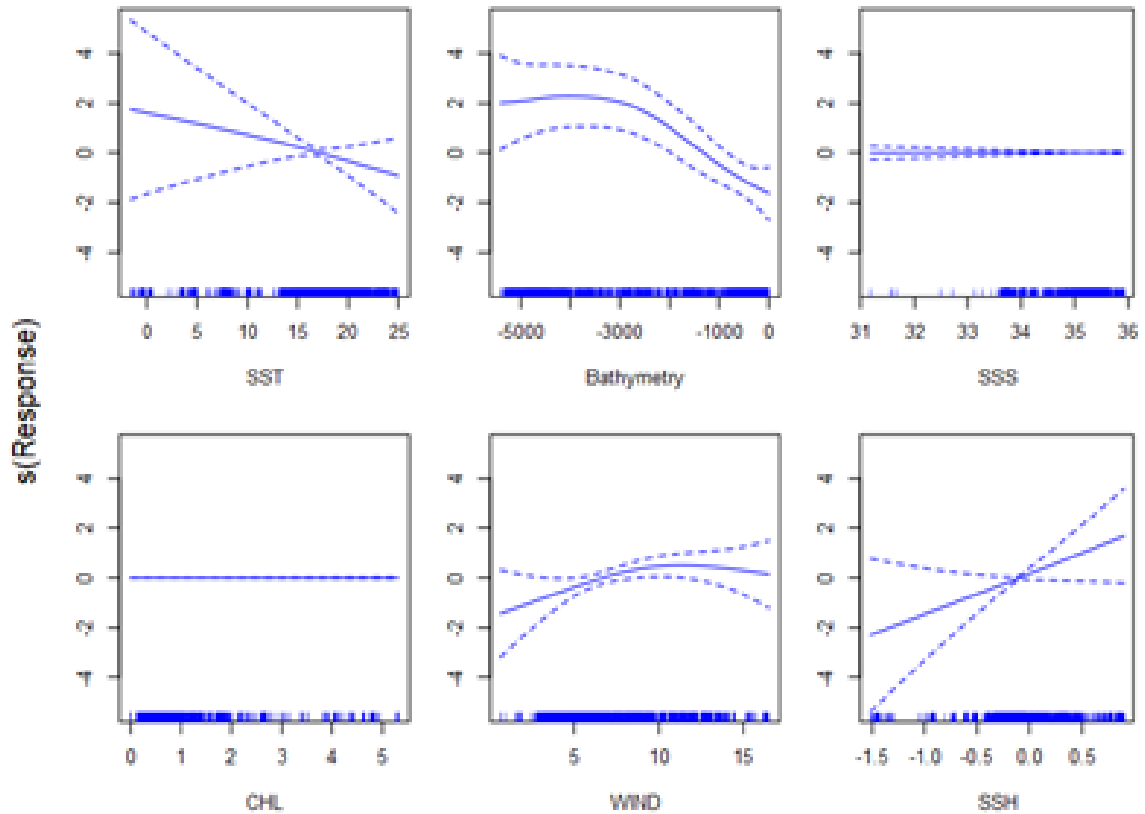

Figure A6: Response curves showing the relationship between the oceanographic variables (sea surface temperature; SST, Wind, Bathymetry, sea surface salinity; SSS, seas surface height; SSH and Chlorophyll-a; CHL) and the probability of occurrence of soft-plumaged petrel 2016 – 2019 (excluding 2020) based on GAM.

Model performance

Table A4: Model diagnostic of observed vs predicted soft-plummaged petrel data deduced from the independent test data for the four models. RMSE (Root mean square error), R2 (Variance explained), Cor (Pearson correlation), AUC (Area under the receiver-operated characteristic curve).

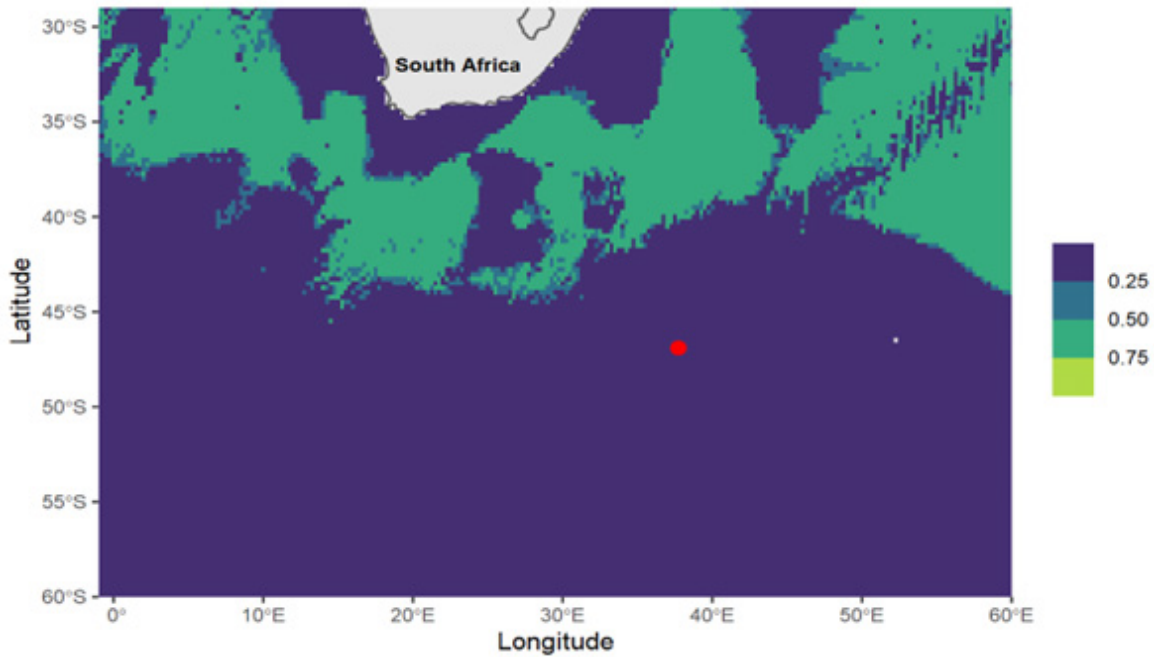| Model	RMSE	R^2	Cor	AUC
GAM	0.23	0.58	0.76	0.96
GLMM	0.27	0.41	0.64	0.92
SPMM	0.23	0.57	0.76	0.96
RF	0.21	0.57	0.75	0.96
Ensemble	0.20	0.60	0.77	0.97

Figure A7: The predicted distribution (probability of occurrence) of soft-plumaged petrels from 2016-2021 (excluding 2020), from ensemble model. The location of the Prince Edward Islands is indicated by the red dot.

Great-winged petrel

Great-winged petrel had no significant relationship with oceanographic variables (p-value> 0.05), except for wind (GAM, edf = 1.06, chi-square = 4.39, p-value = 0.01, adjusted R^2 = 0.29, deviance Explained = 37%, Figures A8 and A9, Table A5) and SSH (GAM, edf = 4.03, chi-square = 12.03, p-value <0.01, adjusted R^2 = 0.29, deviance explained = 437%, Figure A8). There was an increased probability of occurrence with an increase in wind. There was a non-linear relationship between great-winged petrel with SSH.
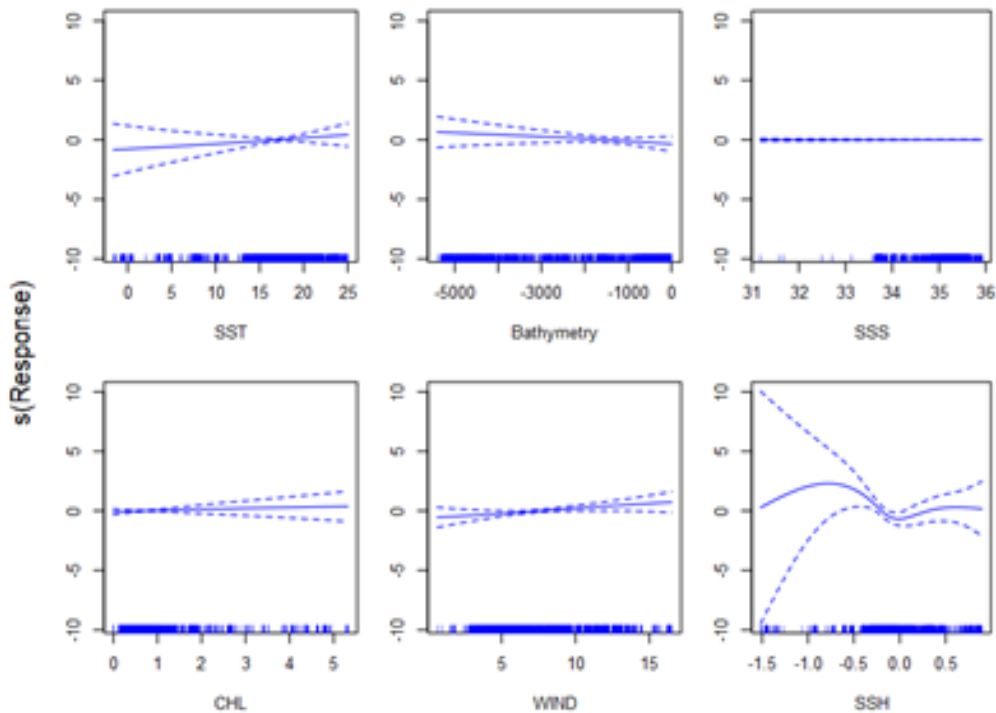

Figure A8: Response curves showing the relationship between the oceanographic variables (sea surface temperature; SST, Wind, Bathymetry, sea surface salinity; SSS, seas surface height; SSH and Chlorophyll-a; CHL) and the probability of occurrence of great-winged petrel 2016 – 2021, excluding 2020.

Table A5:   Model diagnostic of observed vs predicted great-winged petrel data deduced from the independent test data for the four models and ensemble. RMSE (Root mean square error), R2 (Variance explained), Cor (Pearson correlation), AUC (Area under the receiver-operated characteristic curve).

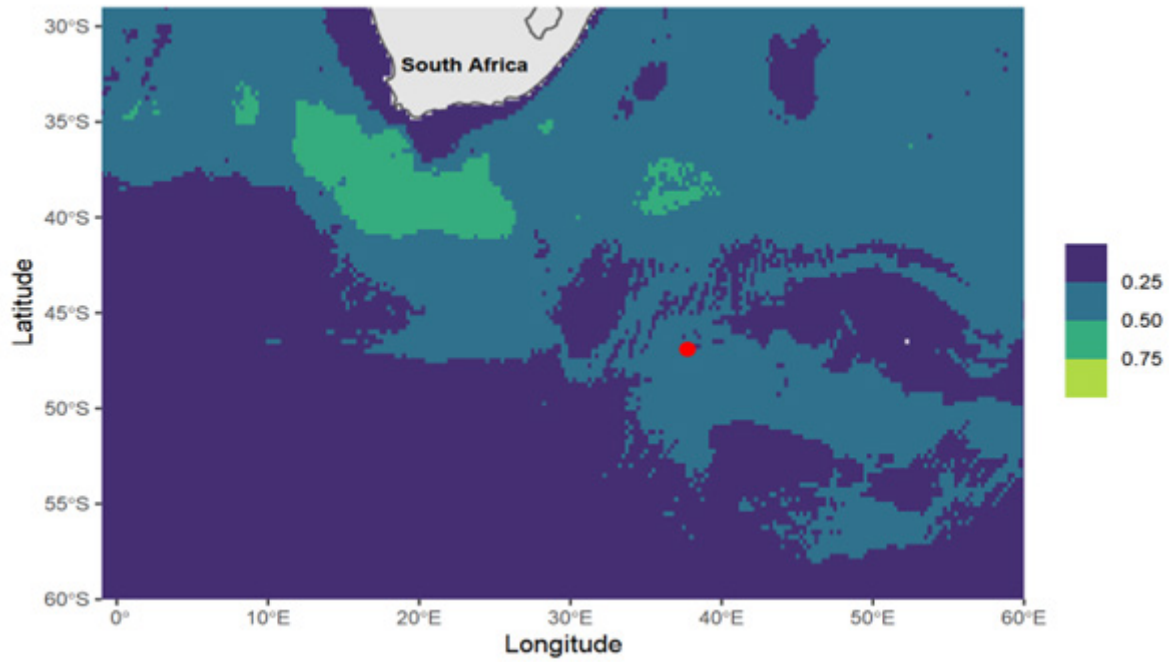| Model	RMSE	R^2	Cor	AUC
GAM	0.26	0.30	0.55	0.90
GLMM	0.30	0.12	0.35	0.72
SPMM	0.27	0.29	0.54	0.88
RF	0.25	0.21	0.46	0.90
Ensemble	0.27	0.22	0.47	0.87

Figure A9:   The predicted distribution (probability of occurrence) of great-winged petrels from 2016-2021 (excluding 2020), from the ensemble model. The location of the Prince Edward Islands is indicated by the red dot.